A semi-implicit scheme for the barotropic primitive equations of atmospheric dynamics

L. Bonaventura and V. Casulli
Dipartimento di Ingegneria Civil ed Ambientale, Università degli Studi di Trento, Mesiano di Povo, Italy and CIRM-ITC, Poro, Italy

Received July 1995
Revised April 1996

Introduction

The hydrostatic primitive equations of atmospheric dynamics in isobaric co-ordinates constitute an initial-boundary value problem with a free surface condition. Most of the numerical weather prediction schemes are based on the primitive equations model. We refer, for instance to[1] for an updated review of these models. Although some numerical models solve the primitive equations directly in pressure co-ordinates (see for example)[2]. most of the present schemes employ terrain following co-ordinates for the vertical discretization. For illustrative purposes, in this paper a reformulation of the primitive equations in the simplified case of a dry, barotropic atmosphere is presented and discussed. The primitive equations in isobaric co-ordinates are rewritten, by expressing the geopotential gradient in terms of the surface pressure gradient. Furthermore, the free surface equation for the atmospheric pressure at the Earth's surface is written in conservative form. In most of the currently used schemes, the sources of instability are handled by using a semi-implicit discretization of the geopotential gradient (e.g.[1,3-6], and the references contained therein). The present approach aims at separating the semi-implicit treatment of the external gravity waves from that of internal gravity waves. As a first step in this direction, a semi-implicit, finite difference algorithm is developed in the case of a barotropic atmosphere, using isobaric co-ordinates instead of terrain following ones. Following the approach used in[7,8], the surface pressure gradient in the momentum equations and the horizontal velocities in the free surface equation are discretized implicitly in time. There results a five-diagonal system of equations for the ground pressure values. Advection and horizontal viscosity terms are discretized by a time-explicit semi-Lagrangian method; vertical viscosity terms are treated implicitly, in order to improve numerical stability. The stability of the resulting scheme depends only on the horizontal viscous terms. Furthermore, the present method is mass conservative and combines the efficiency of the semi-implicit feature (see[9] for a review of semi-Lagrangian, semi-implicit schemes) with a fine resolution of the vertical structure of the flows. Further research is in progress, for the more general case of a baroclinic atmosphere, in order to

International Journal of Numerical Methods for Heat & Fluid Flow Vol. 7 No. 1, 1997, pp. 63-80.

obtain a semi-implicit scheme whose stability is independent on the speed of internal gravity waves.

Reformulation of the 3D primitive equations

The standard form of the primitive equations in pressure co-ordinates is (see e.g.[10,11]):

$$\frac{Du}{Dt} - fv = -\frac{1}{a\cos\theta}\frac{\partial\phi}{\partial\lambda} + \mu\nabla^2 u + \frac{\partial}{\partial p}\left[\nu\frac{\partial u}{\partial p}\right]$$

$$\frac{Dv}{Dt} + fu = -\frac{1}{a}\frac{\partial\phi}{\partial\theta} + \mu\nabla^2 v + \frac{\partial}{\partial p}\left[\nu\frac{\partial v}{\partial p}\right]$$

$$\frac{1}{a\cos\theta}\frac{\partial u}{\partial\lambda} + \frac{1}{\cos\theta}\frac{1}{a}\frac{\partial\left(v\cos\theta\right)}{\partial\theta} + \frac{\partial\omega}{\partial p} = 0 \qquad (1)$$

with the kinematic boundary condition being

$$\frac{\partial\eta}{\partial t} + u(\lambda,\theta,\eta,t)\frac{1}{a\cos\theta}\frac{\partial\eta}{\partial\lambda} + v(\lambda,\theta,\eta,t)\frac{1}{a}\frac{\partial\eta}{\partial\theta} = \omega(\lambda,\theta,\eta,t) \qquad (2)$$

at the Earth's surface and $\omega(\lambda,\theta,0,t) = 0$ at the upper boundary of the atmosphere. Here, (λ, θ) denote the horizontal spherical co-ordinates and p the vertical isobaric co-ordinate, a is the Earth's radius, ϕ is the geopotential, Ω is the Earth's angular velocity, and $f = 2\Omega\sin\theta$ is the Coriolis coefficient. $\eta = \eta(\lambda, \theta, t)$ denotes the pressure at the Earth's surface; the orographic profile is described by a function $h = h(\lambda, \theta)$. The horizontal eddy viscosity coefficient is assumed to be constant and is denoted by μ. The vertical eddy viscosity coefficient is denoted by υ. Following the usual notations, we also set $x = \lambda a\cos\theta$, $y = a\theta$. The velocities are defined as $u = a\cos\theta\frac{d\lambda}{dt}$, $v = a\frac{d\theta}{dt}$, $\omega = \frac{dp}{dt}$ and the Lagrangian derivative is

$$\frac{D}{Dt} = \frac{\partial}{\partial t} + u\frac{1}{a\cos\theta}\frac{\partial}{\partial\lambda} + v\frac{1}{a}\frac{\partial}{\partial\theta} + \omega\frac{\partial}{\partial p}$$

The gradient at constant pressure is denoted by

$$\nabla\psi = \left(\frac{1}{a\cos\theta}\frac{\partial\psi}{\partial\lambda}, \ \frac{1}{a}\frac{\partial\psi}{\partial\theta}\right)$$

and the spherical Laplacian in the horizontal co-ordinates is denoted by

$$\nabla^2\psi = \frac{1}{a^2\cos^2\theta}\frac{\partial^2\psi}{\partial\lambda^2} + \frac{1}{a^2\cos^2\theta}\frac{\partial}{\partial\theta}\left(\cos\theta\frac{\partial\psi}{\partial\theta}\right)$$

By using the equation of state $p = RT\rho$, the hydrostatic assumption is expressed in terms of the geopotential as

$$\frac{\partial\phi}{\partial p} = -\frac{RT}{p} \qquad (3)$$

where R denotes the gas constant, T and ρ denote the absolute temperature and the density, respectively.

In order to express the horizontal gradient of the geopotential in terms of the gradient of η, consider the equation

$$\phi(\lambda,\theta,\eta(\lambda,\theta,t),t)-\phi(\lambda,\theta,p,t)=\int_p^\eta \frac{\partial\phi}{\partial\zeta}(\lambda,\theta,\zeta,t)d\zeta \tag{4}$$

where the geopotential at the Earth's surface is given by

$$gh(\lambda,\theta)=\phi(\lambda,\theta,\eta(\lambda,\theta,t),t)$$

Differentiating (4) with respect to the horizontal variables, by the chain rule one obtains

$$\begin{aligned}\nabla\phi(\lambda,\theta,p,t)&=\nabla\phi(\lambda,\theta,\eta(\lambda,\theta,t),t)-\nabla\int_p^\eta \frac{\partial\phi}{\partial\zeta}(\lambda,\theta,\zeta,t)d\zeta\\
&=g\nabla h(\lambda,\theta)-\frac{\partial\phi}{\partial p}(\lambda,\theta,\eta(\lambda,\theta,t),t)\nabla\eta(\lambda,\theta,t)\\
&\quad-\int_p^\eta \nabla\frac{\partial\phi}{\partial\zeta}(\lambda,\theta,\zeta,t)d\zeta\end{aligned}$$

In an autobarotropic atmosphere, the temperature is assumed to depend on the pressure only, i.e. $T = T(p)$ (see e.g.[12]). In this case, by using equation (3) one obtains

$$\nabla\phi(\lambda,\theta,p,t)=g\nabla h(\lambda,\theta)+R\frac{T(\eta)}{\eta}\nabla\eta \tag{5}$$

Furthermore, the equation for η can be set in conservative form by using the continuity equation and the boundary condition $\omega(\lambda, \theta, 0, t) = 0$. Specifically, from the continuity equation in pressure co-ordinates one has

$$\begin{aligned}\omega(\lambda,\theta,\eta,t)&=\int_0^\eta \frac{\partial\omega}{\partial\zeta}(\lambda,\theta,\zeta,t)d\zeta \qquad (6)\\
&=-\int_0^\eta\left[\frac{1}{a\cos\theta}\frac{\partial u}{\partial\lambda}(\lambda,\theta,\zeta,t)+\frac{1}{\cos\theta}\frac{1}{a}\frac{\partial(v(\lambda,\theta,\zeta,t)\cos\theta)}{\partial\theta}\right]d\zeta\\
&=-\frac{1}{a\cos\theta}\frac{\partial}{\partial\lambda}\left[\int_0^\eta u\,d\zeta\right]-\frac{1}{\cos\theta}\frac{1}{a}\frac{\partial}{\partial\theta}\left[\int_0^\eta v\cos\theta\,d\zeta\right]\\
&\quad+u(\lambda,\theta,\eta,t)\frac{1}{a\cos\theta}\frac{\partial\eta}{\partial\lambda}+v(\lambda,\theta,\eta,t)\frac{1}{a}\frac{\partial\eta}{\partial\theta}\end{aligned}$$

Thus, by using the kinematic conditions (2) one gets the following conservative form for the free surface equation

$$\frac{\partial\eta}{\partial t}+\frac{1}{a\cos\theta}\frac{\partial}{\partial\lambda}\left[\int_0^\eta u\,d\zeta\right]+\frac{1}{\cos\theta}\frac{1}{a}\frac{\partial}{\partial\theta}\left[\int_0^\eta v\cos\theta\,d\zeta\right]=0 \tag{7}$$

The present formulation of the barotropic primitive equations is then given by

$$\frac{Du}{Dt} - fv = -g\frac{1}{a\cos\theta}\frac{\partial h}{\partial\lambda} - \frac{RT(\eta)}{\eta}\frac{1}{a\cos\theta}\frac{\partial\eta}{\partial\lambda} + \mu\nabla^2 u + \frac{\partial}{\partial p}\left[\nu\frac{\partial u}{\partial p}\right]$$
$$\frac{Dv}{Dt} + fu = -g\frac{1}{a}\frac{\partial h}{\partial\theta} - \frac{RT(\eta)}{\eta}\frac{1}{a}\frac{\partial\eta}{\partial\theta} + \mu\nabla^2 v + \frac{\partial}{\partial p}\left[\nu\frac{\partial v}{\partial p}\right] \tag{8}$$
$$\frac{1}{a\cos\theta}\frac{\partial u}{\partial\lambda} + \frac{1}{\cos\theta}\frac{1}{a}\frac{\partial\left(v\cos\theta\right)}{\partial\theta} + \frac{\partial\omega}{\partial p} = 0$$

with the free boundary condition

$$\frac{\partial\eta}{\partial t} + \frac{1}{a\cos\theta}\frac{\partial}{\partial\lambda}\left[\int_0^\eta u d\zeta\right] + \frac{1}{\cos\theta}\frac{1}{a}\frac{\partial}{\partial\theta}\left[\int_0^\eta v\cos\theta d\zeta\right] = 0 \tag{9a}$$

at the Earth's surface $p = \eta$. The dynamical boundary conditions at the Earth's surface are taken to be

$$\nu\frac{\partial u}{\partial p}(\lambda,\theta,\eta,t) = -K\left[u^2(\lambda,\theta,\eta,t) + v^2(\lambda,\theta,\eta,t)\right]^{\frac{1}{2}} u(\lambda,\theta,\eta,t)$$
$$\nu\frac{\partial v}{\partial p}(\lambda,\theta,\eta,t) = -K\left[u^2(\lambda,\theta,\eta,t) + v^2(\lambda,\theta,\eta,t)\right]^{\frac{1}{2}} v(\lambda,\theta,\eta,t) \tag{9b}$$

where K denotes a non-negative drag coefficient. The specific form for of v and K is to be determined from an appropriate turbulence model (see e.g.[13,14]). At the boundary $p = 0$ the dynamic boundary conditions are taken to be

$$\nu\frac{\partial u}{\partial p}(\lambda,\theta,0,t) = 0; \qquad \nu\frac{\partial v}{\partial p}(\lambda,\theta,0,t) = 0 \tag{10}$$

The vertically averaged equations associated to (8) can also be considered. For an atmosphere at constant temperature T the equations for the averaged quantities

$$U(\lambda,\theta,t) = \frac{1}{\eta}\int_0^\eta u(\lambda,\theta,p,t)\,dp; \quad V(\lambda,\theta,t) = \frac{1}{\eta}\int_0^\eta v(\lambda,\theta,p,t)\,dp$$

can be derived by the usual approximations, so that one has

$$\frac{DU}{Dt} - fV = -g\frac{1}{a\cos\theta}\frac{\partial h}{\partial\lambda} - R\frac{T}{\eta}\frac{1}{a\cos\theta}\frac{\partial\eta}{\partial\lambda} + \mu\nabla^2 U - \gamma U$$
$$\frac{DV}{Dt} + fU = -g\frac{1}{a}\frac{\partial h}{\partial\theta} - R\frac{T}{\eta}\frac{1}{a}\frac{\partial\eta}{\partial\theta} + \mu\nabla^2 V - \gamma V \tag{11}$$
$$\frac{\partial\eta}{\partial t} + \frac{1}{a\cos\theta}\frac{\partial\left(U\eta\right)}{\partial\lambda} + \frac{1}{\cos\theta}\frac{1}{a}\frac{\partial\left(V\eta\cos\theta\right)}{\partial\theta} = 0$$

where $\frac{D}{Dt} = \frac{\partial}{\partial t} + U\frac{1}{a\cos\theta}\frac{\partial}{\partial\lambda} + V\frac{1}{a}\frac{\partial}{\partial\theta}$ and γ is a non-negative friction coefficient obtained from vertical averaging. Equations (11) are equivalent to the well-known shallow water equations. In fact, for any pressure value p one has that

$$\eta = p e^{\{\frac{\phi - gh}{RT}\}} \tag{12}$$

Therefore, for $\alpha = \lambda, \theta, t$ there results

$$\frac{\partial \eta}{\partial \alpha} = \frac{p}{RT} e^{\{\frac{\phi - gh}{RT}\}} \frac{\partial(\phi - gh)}{\partial \alpha}$$

and, choosing the reference pressure level p so that log $\frac{\eta}{p} = 1$, the customary shallow water equations are re-obtained.

Semi-implicit discretization of the 3D barotropic model

The barotropic equations (8) are considered at each time t on the domain $\mathrm{D} = [0, 2\pi] \times [-\frac{\pi}{2}, \frac{\pi}{2}] \times [0, \eta(\lambda, \theta, t)]$. Given a maximum pressure value $p_{\max}$, such that $\eta(\lambda, \theta, t) \leq p_{\max}$, a staggered discretization grid with N_p discrete pressure levels $p_{k+\frac{1}{2}}$ is introduced, such that $p_{\frac{1}{2}} = 0$, $p_{N_p+\frac{1}{2}} = p_{\max}$ and $p_{\frac{1}{2}} < \ldots < p_{N_p+\frac{1}{2}}$. For each vertical level k there is an horizontal grid plane with N_x periodically arranged nodes in the λ direction and N_y nodes in the θ direction. Spatial discretization steps are defined as $\Delta\lambda = \frac{2\pi}{N_x}$, $\Delta\theta = \frac{\pi}{N_y}$; $\lambda_i = (i - \frac{1}{2})\Delta\lambda$, $i = 1, \ldots, N_x$, $\theta_j = -\frac{\pi}{2} + (j - \frac{1}{2})\Delta\theta$, $j = 1, \ldots, N_y$, and $\Delta p_k = p_{k+\frac{1}{2}} - p_{k-\frac{1}{2}}$, $k = 1, \ldots, N_p$. We also define the discretization steps in x, y co-ordinates as $\Delta x_j = a\Delta\lambda \cos\theta_j$, $\Delta y = a\Delta\theta$. The horizontal grid planes are arranged as a staggered, C-type discretization grid. Each cell is numbered at its centre with indices i, j and k; The discrete u velocity is then defined at half integer i and integers j and k; v is defined at integers i, k and half integer j; ω is defined at integers i, j and half integers k. Finally η, h are defined at integers i, j (see Figure 1). At points where they are not defined, the

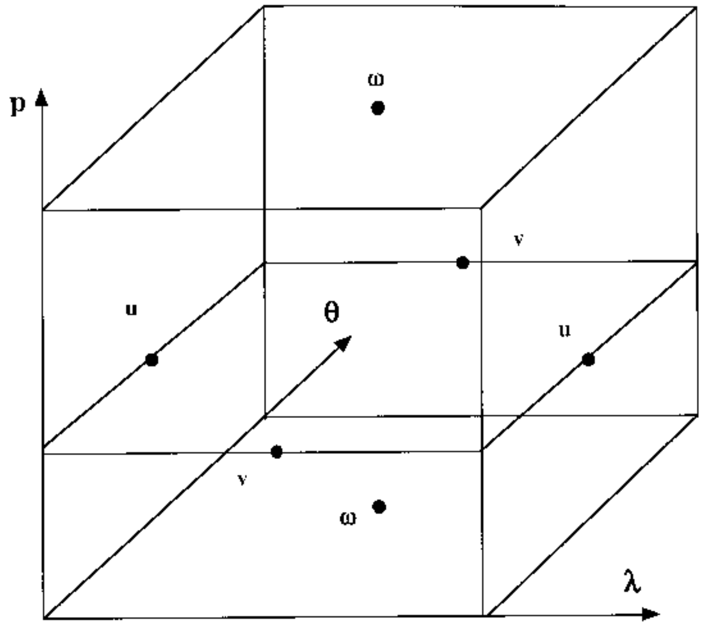

Figure 1.
Grid cell

discrete variables are computed by simple arithmetical mean of the nearest defined values. At each discrete time n, only the cells below the free surface correspond to air parcels above the Earth's surface. The index $k = M^n_{i,j}$ denotes the top cell of the effective computational domain (see Figure 2). Specifically,

$$M^n_{i,j} = \max_{k \leq N_p} \{k : \eta^n_{i,j} > p_{k+\frac{1}{2}}\}$$

Later, for convenience, $M^n_{i,j}$ will be denoted simply by M. Accordingly, the vertical grid spacing at the top layer also depends on the discrete time n and is

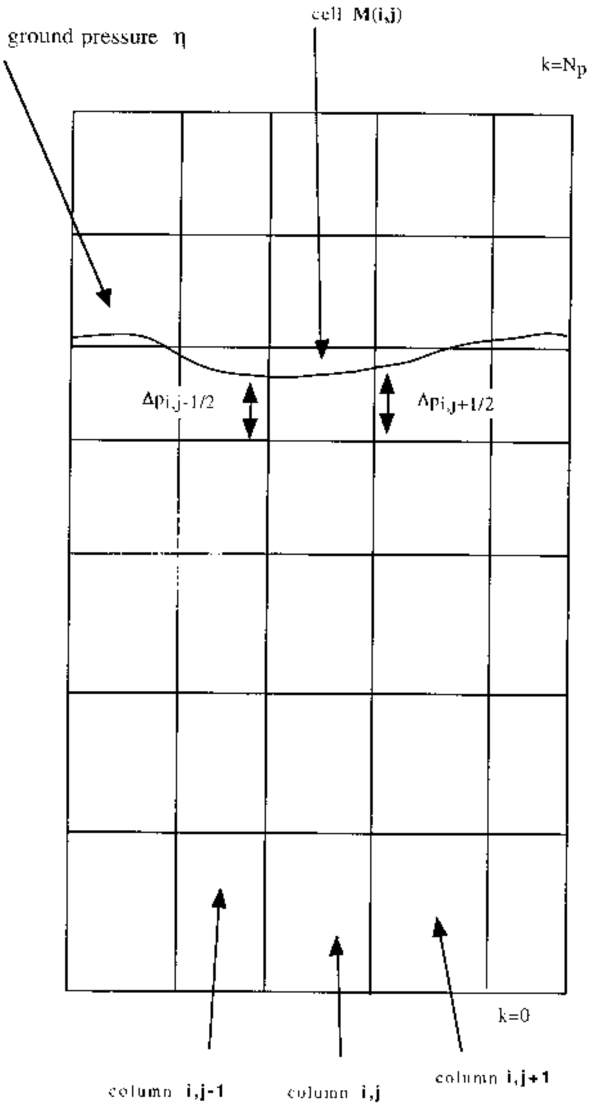

Figure 2.
Vertical grid section

defined as $\Delta p^n_{i,j,M} = \eta^n_{i,j} - p_{M-\frac{1}{2}}$. The resulting computational domain consists of at most $N_x \times N_y \times N_p$ cells. At the South pole cells (j = 1) the velocities $v_{i,\frac{1}{2},k}$ are not defined and never come into play. Similarly, at the North pole cells ($j = N_y$) the velocities $v_{i,N_{y+\frac{1}{2}},k}$ are not needed.

In order to obtain a finite difference scheme whose stability is independent of the free-surface wave speed, the gradient of surface pressure in the momentum equations (8) and the horizontal velocities in the free surface equation (9) are discretized implicitly in time. Furthermore, since we are interested in achieving a relatively fine vertical resolution, the vertical viscosity terms and the friction terms at the Earth's surface will be discretized implicitly as well, in order to improve the stability of the method (see e.g.[15]). It will be shown that, in this way, the stability restrictions for the present method will only depend on the horizontal viscosity.

We denote by $(\mathcal{G}u)^n_{i+\frac{1}{2},j,k}$, $(\mathcal{G}v)^n_{i,j+\frac{1}{2},k}$ the terms discretized explicitly in the momentum equations. These include the semi-Lagrangian discretization of the advection and horizontal viscosity terms, Coriolis terms and orography terms. For a detailed presentation of the semi-Lagrangian methods employed, we refer to[3,7,15]; see also[9] for a more general discussion and[1] for the details of the implementation in spherical geometry.

The semi-implicit discretization of equations (8)-(9) takes then the form

$$u^{n+1}_{i+\frac{1}{2},j,k} = (\mathcal{G}u)^n_{i+\frac{1}{2},j,k} - \frac{RT_M}{\eta^n_{i+\frac{1}{2},j}}\frac{\Delta t}{\Delta x_j}\delta(\eta^{n+1}_{i+1,j} - \eta^{n+1}_{i,j}) + \Delta t\frac{\nu_{k+\frac{1}{2}}\dfrac{u^{n+1}_{i+\frac{1}{2},j,k+1} - u^{n+1}_{i+\frac{1}{2},j,k}}{\Delta p^n_{i+\frac{1}{2},j,k+\frac{1}{2}}} - \nu_{k-\frac{1}{2}}\dfrac{u^{n+1}_{i+\frac{1}{2},j,k} - u^{n+1}_{i+\frac{1}{2},j,k-1}}{\Delta p^n_{i+\frac{1}{2},j,k-\frac{1}{2}}}}{\Delta p^n_{i+\frac{1}{2},j,k}} \tag{13}$$

$$v^{n+1}_{i,j+\frac{1}{2},k} = (\mathcal{G}v)^n_{i,j+\frac{1}{2},k} - \frac{RT_M}{\eta^n_{i,j+\frac{1}{2}}}\frac{\Delta t}{\Delta y}\delta(\eta^{n+1}_{i,j+1} - \eta^{n+1}_{i,j}) + \Delta t\frac{\nu_{k+\frac{1}{2}}\dfrac{v^{n+1}_{i,j+\frac{1}{2},k+1} - v^{n+1}_{i,j+\frac{1}{2},k}}{\Delta p^n_{i,j+\frac{1}{2},k+\frac{1}{2}}} - \nu_{k-\frac{1}{2}}\dfrac{v^{n+1}_{i,j+\frac{1}{2},k} - v^{n+1}_{i,j+\frac{1}{2},k-1}}{\Delta p^n_{i,j+\frac{1}{2},k-\frac{1}{2}}}}{\Delta p^n_{i,j+\frac{1}{2},k}} \tag{14}$$

$$\omega^{n+1}_{i,j,k+\frac{1}{2}} = \omega^{n+1}_{i,j,k-\frac{1}{2}} - \frac{\Delta p^n_{i+\frac{1}{2},j,k}u^{n+1}_{i+\frac{1}{2},j,k} - \Delta p^n_{i-\frac{1}{2},j,k}u^{n+1}_{i-\frac{1}{2},j,k}}{\Delta x_j} - \frac{1}{\cos\theta_j}\frac{\Delta p^n_{i,j+\frac{1}{2},k}v^{n+1}_{i,j+\frac{1}{2},k}\cos\theta_{j+\frac{1}{2}} - \Delta p^n_{i,j-\frac{1}{2},k}v^{n+1}_{i,j-\frac{1}{2},k}\cos\theta_{j-\frac{1}{2}}}{\Delta y} \tag{15}$$

$$
\begin{aligned}
A_j \eta_{i,j}^{n+1} &= A_j \eta_{i,j}^{n} - \delta \Delta t \Delta\theta \Big[\sum_{k=1}^{M} \Delta p_{i+\frac{1}{2},j,k}^{n} u_{i+\frac{1}{2},j,k}^{n+1} - \sum_{k=1}^{M} \Delta p_{i-\frac{1}{2},j,k}^{n} u_{i-\frac{1}{2},j,k}^{n+1} \Big] \\
&- \delta \Delta t \Delta\lambda \Big[\sum_{k=1}^{M} \Delta p_{i,j+\frac{1}{2},k}^{n} v_{i,j+\frac{1}{2},k}^{n+1} \cos\theta_{j+\frac{1}{2}} - \sum_{k=1}^{M} \Delta p_{i,j-\frac{1}{2},k}^{n} v_{i,j-\frac{1}{2},k}^{n+1} \cos\theta_{j-\frac{1}{2}} \Big] \\
&- (1-\delta) \Delta t \Delta\theta \Big[\sum_{k=1}^{M} \Delta p_{i+\frac{1}{2},j,k}^{n} u_{i+\frac{1}{2},j,k}^{n} - \sum_{k=1}^{M} \Delta p_{i-\frac{1}{2},j,k}^{n} u_{i-\frac{1}{2},j,k}^{n} \Big] \qquad (16) \\
&- (1-\delta) \Delta t \Delta\lambda \Big[\sum_{k=1}^{M} \Delta p_{i,j+\frac{1}{2},k}^{n} v_{i,j+\frac{1}{2},k}^{n} \cos\theta_{j+\frac{1}{2}} - \sum_{k=1}^{M} \Delta p_{i,j-\frac{1}{2},k}^{n} v_{i,j-\frac{1}{2},k}^{n} \cos\theta_{j-\frac{1}{2}} \Big]
\end{aligned}
$$

where $A_j = a\left\{\left[\sin\frac{\Delta\theta}{2}\right]/\frac{\Delta\theta}{2}\right\}\Delta\lambda\Delta\theta\cos\theta_j$, $f_j = 2\Omega\cos\theta_j$ and δ is an implicitness parameter. For $\delta = 1$, a completely implicit scheme is obtained. Equations (13)-(15) yield a numerically stable scheme for $\frac{1}{2} \le \delta \le 1$, such that maximum accuracy and efficiency are obtained in the case $\delta = \frac{1}{2}$ (see the discussion in[8]). Use of $\delta = \frac{1}{2}$, however, may generate dispersion waves, and $\delta > \frac{1}{2}$ is usually recommended. Equation (16) is the finite volume discretization of the conservative equation for η. Since $\cos(\theta_1 - \frac{\Delta\theta}{2}) = \cos(\theta_{N_y} + \frac{\Delta\theta}{2}) = 0$, equation (16) does not depend on the value of v at the poles. Thus, this equation is valid for all $j = 1, N_y$. The numerical boundary conditions at the Earth's surface are taken to be

$$
\nu_{M+\frac{1}{2}} \frac{u_{i+\frac{1}{2},j,M+1}^{n+1} - u_{i+\frac{1}{2},j,M}^{n+1}}{\Delta p_{i+\frac{1}{2},j,M+\frac{1}{2}}^{n}} = -K\left[\left(u_{i+\frac{1}{2},j,M}^{n}\right)^2 + \left(v_{i+\frac{1}{2},j,M}^{n}\right)^2\right]^{\frac{1}{2}} u_{i+\frac{1}{2},j,M}^{n+1}
$$

$$
\nu_{M+\frac{1}{2}} \frac{v_{i,j+\frac{1}{2},M+1}^{n+1} - v_{i,j+\frac{1}{2},M}^{n+1}}{\Delta p_{i,j+\frac{1}{2},M+\frac{1}{2}}^{n}} = -K\left[\left(u_{i,j+\frac{1}{2},M}^{n}\right)^2 + \left(v_{i,j+\frac{1}{2},M}^{n}\right)^2\right]^{\frac{1}{2}} v_{i,j+\frac{1}{2},M}^{n+1}
$$

The numerical boundary conditions at the top of the atmosphere are taken to be $\omega_{i,j,\frac{1}{2}} = 0$ and

$$
\nu_{\frac{1}{2}} \frac{u_{i+\frac{1}{2},j,1}^{n+1} - u_{i+\frac{1}{2},j,0}^{n+1}}{\Delta p_{i+\frac{1}{2},j,\frac{1}{2}}^{n}} = 0; \quad \nu_{\frac{1}{2}} \frac{v_{i,j+\frac{1}{2},1}^{n+1} - u_{i,j+\frac{1}{2},0}^{n+1}}{\Delta p_{i,j+\frac{1}{2},\frac{1}{2}}^{n}} = 0 \qquad (17)
$$

In the particular case $N_p = 1$ one has $\Delta p_1 = \eta^n$, so that equations (13)-(15) yield a semi-implicit scheme consistent with the vertically averaged equations (11). An analogous two-dimensional scheme on the sphere has been presented in[16].

Solution algorithm

Equations (13)-(16) constitute a linear system of at most $N_x N_y (3N_p + 1)$ equations. In order to compute $u_{i+\frac{1}{2},j,k}^{n+1}$, $v_{i,j+\frac{1}{2},k}^{n+1}$, $\omega_{i,j,k+\frac{1}{2}}^{n+1}$ and $\eta_{i,j}^{n+1}$, such a system has to be solved at each discrete timestep. The number of unknowns is rather large even for coarse grids. By setting $N_x = N_y = N_p = 100$, for example, a system of 3.010.000 equations in 3.010.000 unknowns is obtained. Therefore, equations (13)-(16) are decoupled, so that their solution can be reduced to the solution of a set of simpler linear systems. Specifically, using the matrix notation and defining the vectors ΔP, U, V, $\mathcal{G}$U, $\mathcal{G}$V as

$$\Delta \mathbf{P}^n = \begin{pmatrix} \Delta p_M^n \\ \Delta p_{M-1}^n \\ \vdots \\ \Delta p_1 \end{pmatrix}, \quad \mathbf{U}^{n+1}_{i+\frac{1}{2},j} = \begin{pmatrix} u^{n+1}_{i+\frac{1}{2},j,M} \\ u^{n+1}_{i+\frac{1}{2},j,M-1} \\ \vdots \\ u^{n+1}_{i+\frac{1}{2},j,1} \end{pmatrix}, \quad \mathbf{V}^{n+1}_{i,j+\frac{1}{2}} = \begin{pmatrix} v^{n+1}_{i,j+\frac{1}{2},M} \\ v^{n+1}_{i,j+\frac{1}{2},M-1} \\ \vdots \\ v^{n+1}_{i,j+\frac{1}{2},1} \end{pmatrix}$$

$$(\mathcal{G}\mathbf{U})^n_{i+\frac{1}{2},j} = \begin{pmatrix} \Delta p_M (\mathcal{G}u)^n_{i+\frac{1}{2},j,M} \\ \Delta p_{M-1} (\mathcal{G}u)^n_{i+\frac{1}{2},j,M-1} \\ \vdots \\ \Delta p_1 (\mathcal{G}u)^n_{i+\frac{1}{2},j,1} \end{pmatrix}, \quad (\mathcal{G}\mathbf{V})^n_{i,j+\frac{1}{2}} = \begin{pmatrix} \Delta p_M (\mathcal{G}v)^n_{i,j+\frac{1}{2},M} \\ \Delta p_{M-1} (\mathcal{G}v)^n_{i,j+\frac{1}{2},M-1} \\ \vdots \\ \Delta p_1 (\mathcal{G}v)^n_{i,j+\frac{1}{2},1} \end{pmatrix}$$

and the tridiagonal, positive definite matrix

$$\mathbf{A} = \begin{pmatrix} \Delta p_M + a_{M-\frac{1}{2}} + \gamma \Delta t & -a_{M-\frac{1}{2}} & & 0 \\ -a_{M-\frac{1}{2}} & \Delta p_{M-1} + a_{M-\frac{1}{2}} + a_{M-\frac{3}{2}} & -a_{M-\frac{3}{2}} & \\ \cdot & \cdot & \cdot & \\ & \cdot & \cdot & \cdot \\ 0 & & -a_{1+\frac{1}{2}} & \Delta p_1 + a_{\frac{3}{2}} \end{pmatrix}$$

where $a_k = \upsilon_k \frac{\Delta t}{\Delta p k}$ and

$$\gamma_{i+\frac{1}{2},j} = K \left[\left(u_{i+\frac{1}{2},j,M} \right)^2 + \left(v_{i+\frac{1}{2},j,M} \right)^2 \right]^{\frac{1}{2}}$$

equations (13), (14) and (16) are written in the following matrix form

$$\mathbf{A}^n_{i+\frac{1}{2},j} \mathbf{U}^{n+1}_{i+\frac{1}{2},j} = (\mathcal{G}\mathbf{U})^n_{i+\frac{1}{2},j} - \delta \frac{RT_M}{\eta^n_{i+\frac{1}{2},j}} \frac{\Delta t}{\Delta x_j} (\eta^{n+1}_{i+1,j} - \eta^{n+1}_{i,j}) \boldsymbol{\Delta} \mathbf{P}^n_{i+\frac{1}{2},j} \qquad (18)$$

$$\mathbf{A}^n_{i,j+\frac{1}{2}} \mathbf{V}^{n+1}_{i,j+\frac{1}{2}} = (\mathcal{G}\mathbf{V})^n_{i,j+\frac{1}{2}} - \delta \frac{RT_M}{\eta^n_{i,j+\frac{1}{2}}} \frac{\Delta t}{\Delta y} (\eta^{n+1}_{i,j+1} - \eta^{n+1}_{i,j}) \boldsymbol{\Delta} \mathbf{P}^n_{i,j+\frac{1}{2}} \qquad (19)$$

$$\mathcal{A}_j \eta^{n+1}_{i,j} = \mathcal{A}_j \eta^n_{i,j} + \psi^n_{i,j} - \delta \Delta t \Delta \theta \left[\left(\boldsymbol{\Delta} \mathbf{P}^n_{i+\frac{1}{2},j} \right)^T \mathbf{U}^{n+1}_{i+\frac{1}{2},j} - \left(\boldsymbol{\Delta} \mathbf{P}^n_{i-\frac{1}{2},j} \right)^T \mathbf{U}^{n+1}_{i-\frac{1}{2},j} \right]$$

$$-\delta\Delta t\Delta\lambda\left[\left(\Delta\mathbf{P}^{n}_{i,j+\frac{1}{2}}\right)^{T}\mathbf{V}^{n+1}_{i,j+\frac{1}{2}}\cos\theta_{j+\frac{1}{2}}-\left(\Delta\mathbf{P}^{n}_{i,j-\frac{1}{2}}\right)^{T}\mathbf{V}^{n+1}_{i,j-\frac{1}{2}}\cos\theta_{j-\frac{1}{2}}\right] \quad (20)$$

where

$$\psi^{n}_{i,j}=-(1-\delta)\Delta t\Delta\theta\left[\left(\Delta\mathbf{P}^{n}_{i+\frac{1}{2},j}\right)^{T}\mathbf{U}^{n}_{i+\frac{1}{2},j}-\left(\Delta\mathbf{P}^{n}_{i-\frac{1}{2},j}\right)^{T}\mathbf{U}^{n}_{i-\frac{1}{2},j}\right]$$
$$-(1-\delta)\Delta t\Delta\lambda\left[\left(\Delta\mathbf{P}^{n}_{i,j+\frac{1}{2}}\right)^{T}\mathbf{V}^{n}_{i,j+\frac{1}{2}}\cos\theta_{j+\frac{1}{2}}-\left(\Delta\mathbf{P}^{n}_{i,j-\frac{1}{2}}\right)^{T}\mathbf{V}^{n}_{i,j-\frac{1}{2}}\cos\theta_{j-\frac{1}{2}}\right]$$

For each i, j the linear equations (18) and (19) for $U^{n+1}_{i\pm\frac{1}{2},j}$ and $V^{n+1}_{i,j\pm\frac{1}{2}}$ are inverted formally to obtain

$$\mathbf{U}^{n+1}_{i+\frac{1}{2},j}=\mathbf{A}^{-1}(\mathcal{G}\mathbf{U})^{n}_{i+\frac{1}{2},j}-\delta\frac{RT_M}{\eta^{n}_{i+\frac{1}{2},j}}\frac{\Delta t}{\Delta x_j}(\eta^{n+1}_{i+1,j}-\eta^{n+1}_{i,j})\mathbf{A}^{-1}\Delta\mathbf{P}^{n}_{i+\frac{1}{2},j}$$

$$\mathbf{V}^{n+1}_{i,j+\frac{1}{2}}=\mathbf{A}^{-1}(\mathcal{G}\mathbf{V})^{n}_{i,j+\frac{1}{2}}-\delta\frac{RT_M}{\eta^{n}_{i,j+\frac{1}{2}}}\frac{\Delta t}{\Delta y}(\eta^{n+1}_{i,j+1}-\eta^{n+1}_{i,j})\mathbf{A}^{-1}\Delta\mathbf{P}^{n}_{i,j+\frac{1}{2}}$$

These expressions are used in equation (20) in order to eliminate for $U^{n+1}_{i\pm\frac{1}{2},j}$ and $V^{n+1}_{i,j\pm\frac{1}{2}}$, so that for each i, j the following equation for $\eta^{n+1}_{i,j}$ results:

$$\left[\mathcal{A}_j+\alpha^{n}_{i+\frac{1}{2},j}+\alpha^{n}_{i-\frac{1}{2},j}+\beta^{n}_{i,j+\frac{1}{2}}+\beta^{n}_{i,j-\frac{1}{2}}\right]\eta^{n+1}_{i,j}$$
$$-\alpha^{n}_{i+\frac{1}{2},j}\eta^{n+1}_{i+1,j}-\alpha^{n}_{i-\frac{1}{2},j}\eta^{n+1}_{i-1,j}-\beta^{n}_{i,j+\frac{1}{2}}\eta^{n+1}_{i,j+1}-\beta^{n}_{i,j-\frac{1}{2}}\eta^{n+1}_{i,j-1}$$
$$=\mathcal{F}^{n}_{i,j} \quad (21)$$

where

$$\mathcal{F}^{n}_{i,j}=\mathcal{A}_j\eta^{n}_{i,j}$$
$$-(1-\delta)\Delta t\Delta\theta\left[\left(\Delta\mathbf{P}^{n}_{i+\frac{1}{2},j}\right)^{T}\mathbf{A}^{-1}(\mathcal{G}\mathbf{U})^{n}_{i+\frac{1}{2},j}-\left(\Delta\mathbf{P}^{n}_{i-\frac{1}{2},j}\right)^{T}\mathbf{A}^{-1}(\mathcal{G}\mathbf{U})^{n}_{i+\frac{1}{2},j}\right]$$
$$-(1-\delta)\Delta t\Delta\lambda\left[\left(\Delta\mathbf{P}^{n}_{i,j+\frac{1}{2}}\right)^{T}\mathbf{A}^{-1}(\mathcal{G}\mathbf{V})^{n}_{i,j+\frac{1}{2}}\cos\theta_{j+\frac{1}{2}}\right.$$
$$\left.-\left(\Delta\mathbf{P}^{n}_{i,j-\frac{1}{2}}\right)^{T}\mathbf{A}^{-1}(\mathcal{G}\mathbf{V})^{n}_{i,j+\frac{1}{2}}\cos\theta_{j-\frac{1}{2}}\right]$$

and α, β are defined as

$$\alpha^{n}_{i+\frac{1}{2},j}=\frac{RT_M}{\eta^{n}_{i+\frac{1}{2},j}}\frac{\delta^2\Delta t^2\Delta\theta}{\Delta x_j}(\Delta\mathbf{P}^{n}_{i+\frac{1}{2},j})^{T}\mathbf{A}^{-1}_{i+\frac{1}{2},j}\Delta\mathbf{P}^{n}_{i+\frac{1}{2},j}$$

$$\beta^{n}_{i,j+\frac{1}{2}}=\frac{RT_M}{\eta^{n}_{i,j+\frac{1}{2}}}\frac{\delta^2\Delta t^2\Delta\lambda}{\Delta y}(\Delta\mathbf{P}^{n}_{i,j+\frac{1}{2}})^{T}\mathbf{A}^{-1}_{i,j+\frac{1}{2}}\Delta\mathbf{P}^{n}_{i,j+\frac{1}{2}}\cos\theta_{j+\frac{1}{2}}$$

Since A is positive definite, A^{-1} is also positive definite, so that it follows

$$(\Delta P)^T A^{-1} \Delta P \geq 0$$

Consequently, equation (21) forms a symmetric, positive definite, diagonally dominant five-diagonal system of $N_x N_y$ equations. The solution of (21) is calculated by a preconditioned conjugate gradient method. A simple diagonal preconditioning has been used in the implementation; furthermore, the two-colour structure of the five-diagonal matrix has been exploited (see for example[17]).

Once the surface pressure at time $n + 1$ has been determined, equations (18) and (19) constitute two $N_x N_y$ tridiagonal linear systems of at most N_p equations each. Such systems are independent, symmetric, diagonally dominant and positive definite. Thus, they can be efficiently solved by a direct method to compute $U^{n+1}_{i\pm\frac{1}{2},j}$ and $V^{n+1}_{i,j\pm\frac{1}{2}}$. Finally, for each cell column the vertical velocities $\omega^{n+1}_{i,j,k+\frac{1}{2}}$, $k = 1, \ldots, M$, are computed from the discretized continuity equation (15), by using the known values of $U^{n+1}_{i\pm\frac{1}{2},j}$ and $V^{n+1}_{i,j\pm\frac{1}{2},k}$ and the boundary condition $\omega^{n+1}_{i,j,\frac{1}{2}} = 0$.

At each time step the computation of the solutions of (13)-(15) is then summarized as follows:

(1) compute the explicit terms $(\mathbf{G}U)^n_{i+\frac{1}{2},j}$ and $(\mathbf{G}V)^n_{i,j+\frac{1}{2}}$;

(2) solve the five-diagonal system (21) to compute η^{n+1};

(3) solve the 2 $N_x N_y$ tridiagonal systems (18) and (19) to compute U^{n+1}, V^{n+1};

(4) compute ω^{n+1} from the discretized continuity equation (1 5).

Stability analysis and numerical results

On a flat, periodic domain in Cartesian co-ordinates, the von Neumann stability analysis for the present model in the linear case can be carried through along the same lines as that in[8] for the analogous 3-D shallow water model. Furthermore, a linear stability analysis in L^2 norm in spherical co-ordinates has been carried out in[18] for the fully implicit scheme ($\delta = 1$). As in[8], one can conclude that the present scheme is unconditionally stable with respect to surface gravity waves and vertical viscosity terms. The only stability constraint on the time step is due to the discretization of the horizontal viscosity terms and is given by

$$\Delta t \leq \left[2\mu\left(\frac{1}{\Delta x_1{}^2} + \frac{1}{\Delta y^2}\right)\right]^{-1}$$

from which it follows that this method becomes unconditionally stable in the absence of horizontal viscosity.

Some preliminary tests on the present numerical scheme have been carried out for various large scale atmospheric flows. Simple linear interpolation has been used for the semi-Lagrangian advection, and the simplest possible preconditioner has been used for the solution of the five-diagonal system for η. The test cases considered here arise from Tests numbers 2 and 6 in[19] for the shallow water equations on the sphere. Such tests have been adapted to equations (11), and the 3-D model has been run with either one or more vertical layers. The initial values for the 500mb geopotential have been transformed into the corresponding initial values for η by using the hydrostatic equation (12) in the case of an isothermal atmosphere, and the same initial velocity fields as in[19] have been used. In all the tests the parameter δ was taken to be equal to 0.55.

The scheme is effectively mass conservative, relative changes in the value of $\int\int \eta(\lambda, \theta, t) \cos\theta d\lambda d\theta$ being of the order of 10^{-12} over 30 days of simulation of a stationary flow with a timestep of one hour.

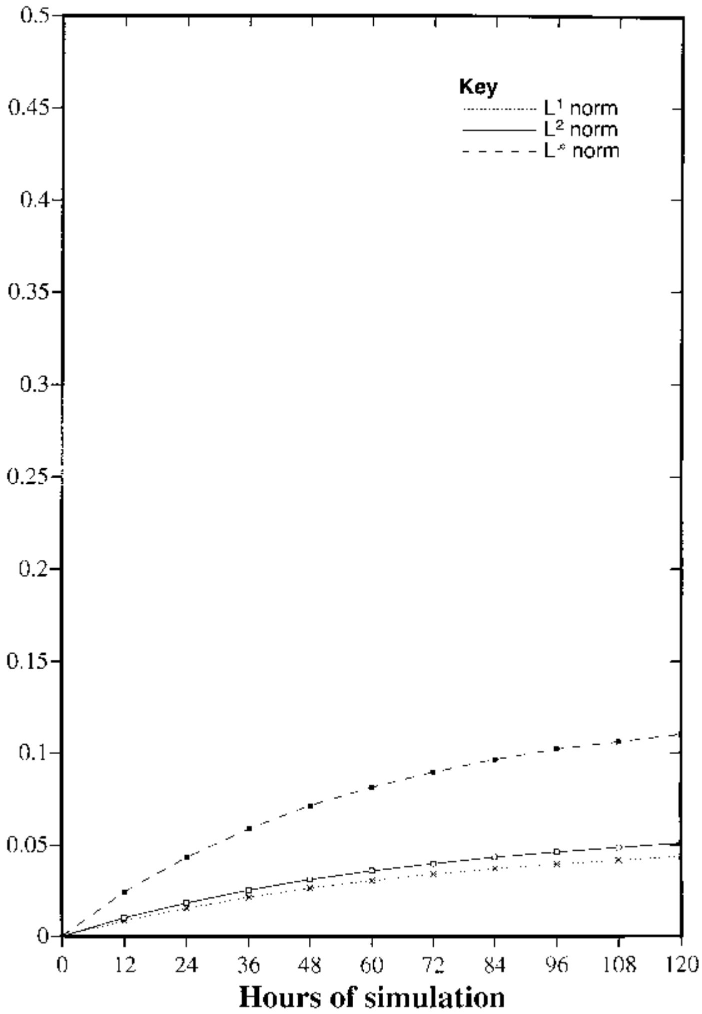

Figure 3.
Relative errors on η in L^1 norm (dotted line), L^2 norm (full line) and L^∞ norm (dashed line) for a zonal flow rotated by $\pi/2$, 720×360 gridpoints, Δt = 1,800s

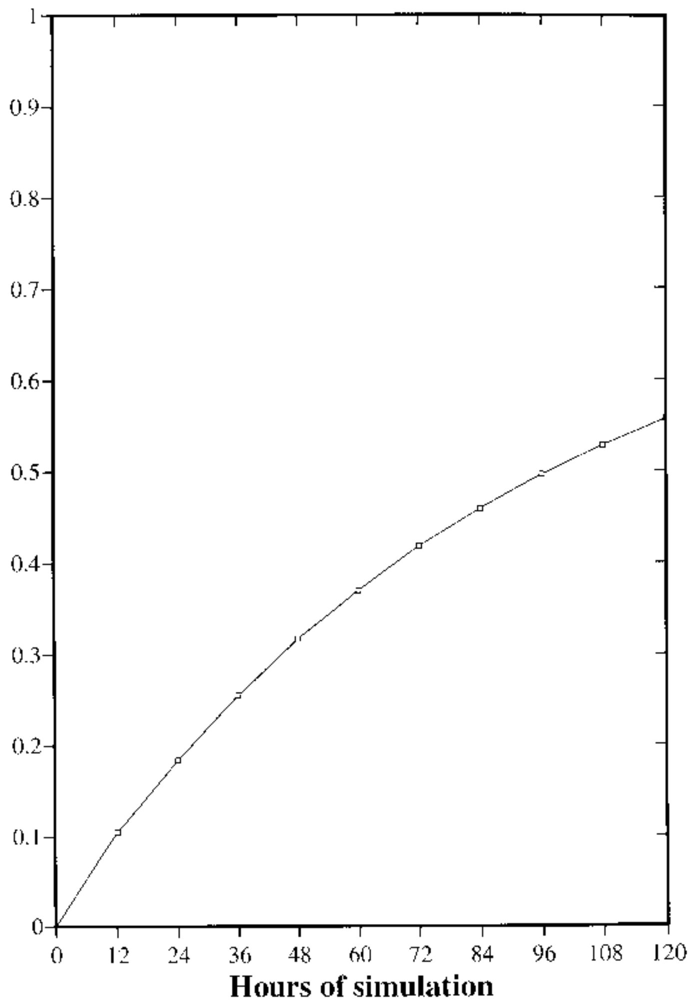

Figure 4.
Relative error on (u, v) in L^2 norm for a zonal flow rotated by $\pi/2$, 720×360 gridpoints, Δt = 1,800s

Relative errors in L^1, L^2, L^∞ norms for the values of η with respect to the known analytical solution of Test 2 for a zonal flow rotated by an angle $\frac{\pi}{2}$ are shown in Figure 3. Figure 4 shows the relative error in L^2 norm for the velocities. The model was run in this case with only one vertical layer on a 720×360 grid with a timestep of 1,800s. The temperature was taken to be T = 273°K throughout, and a purely inviscid flow ($\mu = \upsilon = K = 0$) was considered. The initial flow field for the same rotation angle is shown in Figure 5, and Figure 6 shows the resulting velocities at t = 2 days, as obtained from a simulation with only one vertical layer on a 180×90 grid with a timestep of 3,600s. In Figures 7-9 the flow fields for Test 6 are shown, as computed at times t = 0, 1, 2 days in a simulation with only one vertical layer on a 180×90 grid with a timestep of 1,800s. In

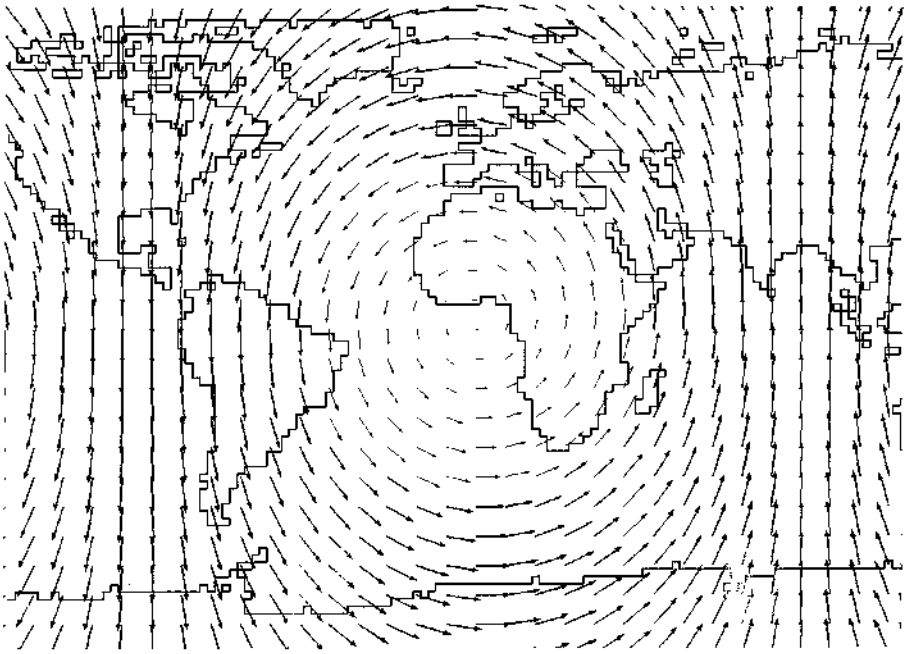

Figure 5.
Zonal flow rotated by $\pi/2$ at $t = 0$, 180×90 gridpoints

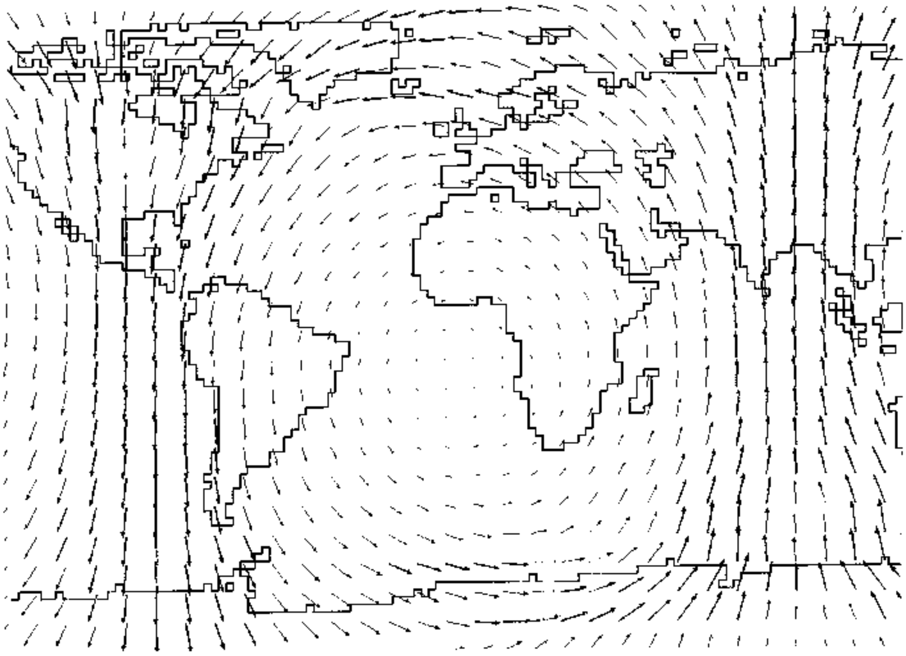

Figure 6.
Zonal flow rotated by $\pi/2$ at $t = 48$ hours, 180×90 gridpoints, $\Delta t = 3{,}600s$

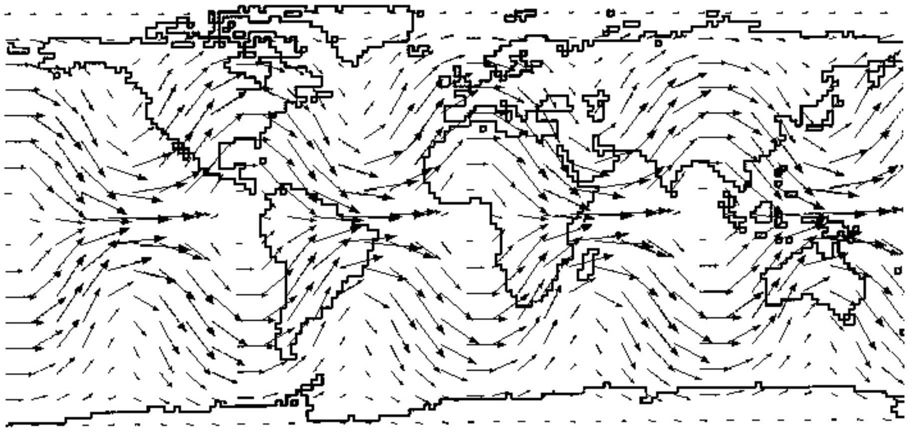

Figure 7. Rossby wave flow field at t = 0, 180 × 90 gridpoints

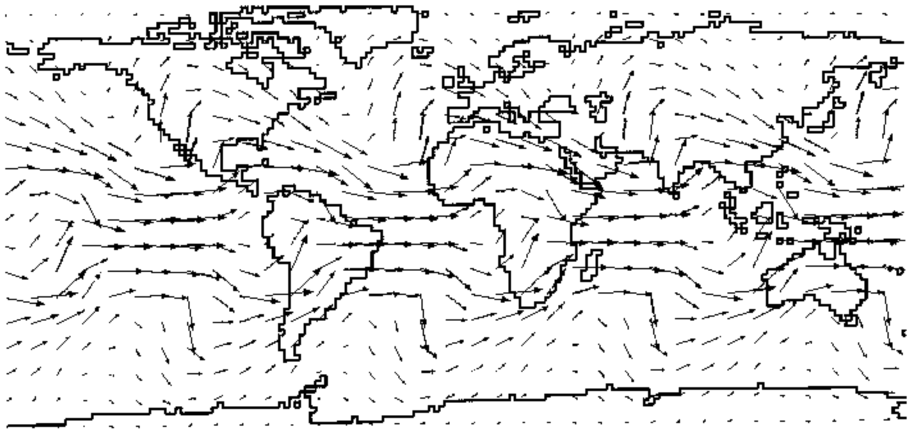

Figure 8. Rossby wave flow field at t = 24 hours, 180 × 90 gridpoints, Δt = 1,800s

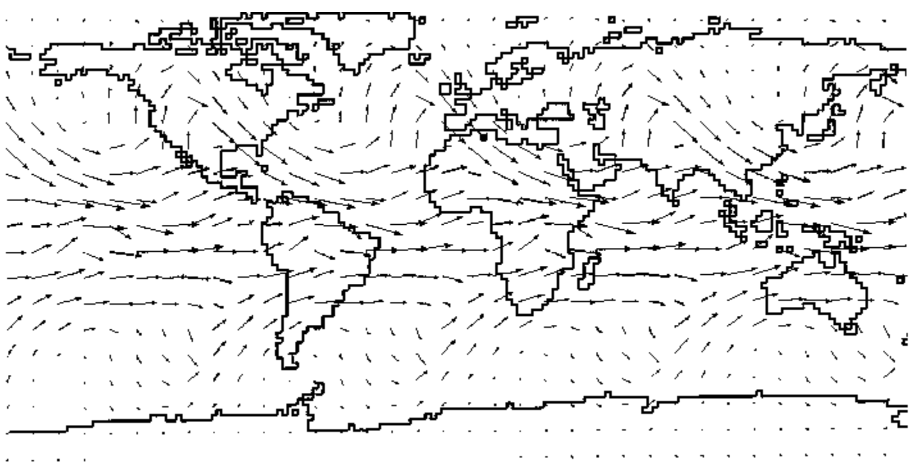

Figure 9. Rossby wave flow field at t = 48 hours, 180 × 90 gridpoints, Δt = 1,800s

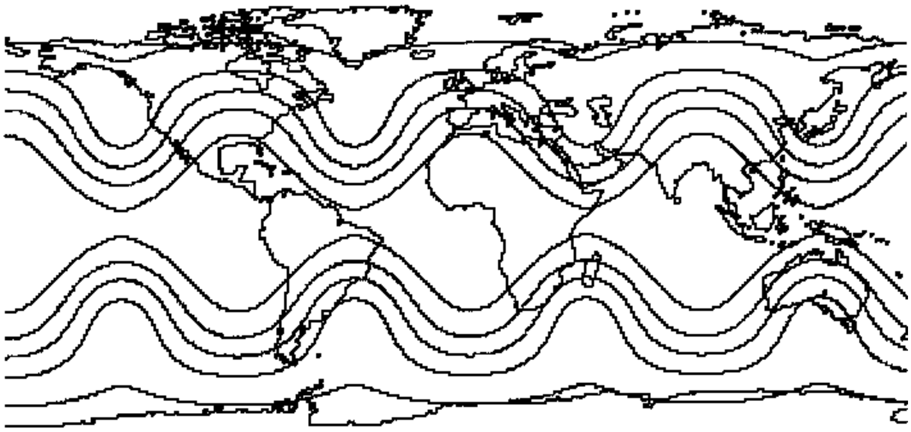

Figure 10.
Rossby wave pressure field at $t = 0$, 360×180 gridpoints

Figures 10 and 11 the isolines of η for Test 6 are shown at times $t = 0$ and $t = 5$ days, respectively, as obtained from a simulation with five vertical layers on a 360×180 grid with a timestep of 600s. In this case, the vertical viscosity and momentum drag coefficients have been taken from[14].

Although the present implementation of the model cannot compete with high accuracy spectral models on tests with simple geometry (for example the corresponding results in[20]), the main features of such large scale flows are well reproduced. Specifically, it can be noted that the four-wave structure of the initial configuration in Test 6 is preserved, which is one of the necessary requirements discussed in[20] for a shallow water solver.

In order to test the performance of the model, a three-dimensional test with the initial data of Test 6 has been performed on an ALPHA AXP 21064 (which allows for 181.6 SPECfp92) using a horizontal grid with 360×180 gridpoints, 40 vertical levels and a 900s timestep. The CPU time needed for a one-day

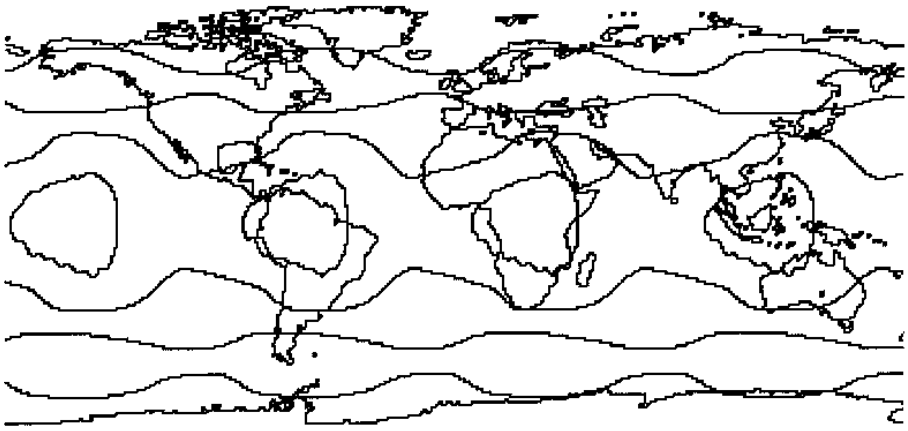

Figure 11.
Rossby wave pressure field at $t = 5$ days 360×180 gridpoints, $\Delta t = 600s$

simulation was approximately 2 hours 45 minutes, thus showing that the model allows for fine vertical resolution at relatively low computational costs.

Conclusions

The present finite difference, semi-implicit, semi-Lagrangian scheme captures the main dynamical features of barotropic atmospheric motion. Given the necessary refinements, it can be regarded as the kernel of a complete baroclinic model. Further work is in progress to handle internal gravity waves within the same framework, as well as to consider heat sources, water vapour transport and regional scale test problems.

Acknowledgements

This paper is the outcome of the first named author's PhD thesis in Mathematics. We would like to thank A. Staniforth, U. Amato and M.E Carfora for many useful comments.

References

1. Hortal, M., "Formulation of the ECMWF model", in *Seminar Proceedings on Numerical Methods in Atmospheric Models*, European Centre for Medium Range Weather Forecasts, Reading, 1991.
2. Leith, C.E., "Numerical simulation of the Earth's atmosphere", in Alder, B., Fernbach, S. and Rotenberg, M. (Eds), *Methods in Comp. Phys. – Appl. in Hydrodynamics*, Vol. 4, Academic Press, New York, NY and London, 1965, pp. 1-29.
3. Casulli, V., "Semi-implicit finite difference methods for the two-dimensional shallow-water equation", *Journal of Comp. Phys.*, Vol. 86, 1990, pp. 56-74.
4. Côté, J. and Staniforth, A., "An accurate and efficient finite-element global model of the shallow water equations, semi-Lagrangian finite-element global model of the shallow water equations", *Monthly Weather Review*, Vol. 18, 1990, pp. 2707-17.
5. Elvius, T. and Sundstrom, A., "Computationally efficient schemes for shallow water equations", *Tellus*, Vol. 25, 1973, pp. 132-56.
6. Robert, A.A., "Semi-Lagrangian and semi-implicit scheme for primitive equations", *Journal of the Meteorological Society of Japan,* Vol. 60, 1982, pp. 319-24.
7. Casulli, V. and Cheng, R.T., "Semi-implicit finite difference methods for three-dimensional shallow water flow", *International Journal for Numerical Methods in Fluids,* Vol. 15, 1992, pp. 629-48.
8. Casulli, V. and Cattani, E., "Stability, accuracy and efficiency of a semi-implicit method for three-dimensional shallow water flow", *Computers & Mathematics with Applications*, Vol. 27, 1994, pp. 99-112.
9. Staniforth, A. and Côté, J., "Semi-Lagrangian integration schemes for atmospheric models – a review", *Monthly Weather Review*, Vol. 119, 1991, pp. 2206-23.
10. Dutton, J.A., *The Ceaseless Wind*, Dover Publications, New York, NY, 1986.
11. Holton, J.R, *An Introduction to Dynamic Meteorology,* Academic Press, Orlando, FL, 1979.
12. Gill, A.E., *Atmosphere-Ocean Dynamics*, Academic Press, San Diego, CA, 1982.
13. Haltiner, G.J. and Williams, R.T., *Numerical Prediction and Dynamic Meteorology*, 2nd ed., Wiley, New York, NY, 1980.
14. Louis, J.E., Tiedke, M. and Geleyn, J.E., "A short history of operational PBL parameterization at ECMWF", in *Proceedings of the ECMWF Workshop on PBL,* 1981, pp. 59-79.

15. Casulli, V. and Bertolazzi, E., "Semi-implicit numerical methods for convection-diffusion equations", in Ciarlini, P. *et al.* (Eds), *Proceedings of the Workshop – Advanced Mathematical Tools in Metrology*, World Scientific, Singapore, 1994, pp. 57-66.
16. Amato, U. and Carfora, M.F., "An unconditionally stable method for the shallow water model in the atmosphere", *Rapporto Interno*, Istituto Applicazioni della Matematica del CNR, Napoli, 1994.
17. Poole, E.L. and Ortega, J.M., "Multicolor ICCG methods for vector computers", *SIAM Journal. of Num. Anal.,* Vol. 24 No. 6, 1987, pp. 1398-419.
18. Bonaventura, L., "Studio analitico e numerico di un modello di equazioni primitive per la dinamica atmosferica", PhD thesis in mathematics, UTM PhDTS, Vol. 1 No. 5, University of Trento, Italy, 1995.
19. Williamson, D.L., Drake, J.B., Hack, J.J., Jakob, R. and Swartztrauber, P.N., "A standard test set for numerical approximations to the shallow water equations in spherical geometry", *Journal. of Comp. Phys.*, Vol. 102, 1992, pp. 211-24.
20. Jakob-Chien, R., Hack, J.J. and Williamson, D.L., "Spectral transform solutions to the shallow water test set", *Journal of Comp. Phys.*, Vol. 119, 1995, pp. 164-87.